Proceedings of the Fifth International Symposium
on
Advanced Nuclear Energy Research
NEUTRONS AS MICROSCOPIC PROBES

P−203

NEUTRON DIFFRACTION FROM LEAD GERMANATE GLASSES

°Norimasa UMESAKI, *Thierry M. BRUNIER, *Adrain C. WRIGHT,
**Alex C. HANNON and ***Rojer N. SCINCLAIR

O Government Industrial Research Institute, Osaka
1-8-31, Midorigaoka, Ikeda, Osaka 563, Japan

* J. J. Thomson Physical Laboratory, Reading University
Whiteknights, Reading RG6 2AF, U.K.

** ISIS Science Division, Rutherford Appleton Laboratory
Chilton, Didcot, Oxon OX11 0QX, U.K.

*** Industrial Technology, Harwell Laboratory
Chilton, Didcot, Oxon OX11 0RA, U.K.

ABSTRACT

High resolution neutron diffraction data have been collected on the PbO-GeO_2 glasses and on GeO_2 for comparison. These neutron data have revealed the existence of 6-fold coordinated germanium (GeO_6 octahedra) by virtue of the shift in the first peak in the obtained total correlation function T(r) and increase in the coordination. The neutron results also indicate that PbO exits as PbO_4 pyramids, as found in the orthorhombic form of PbO crystal, in the studied PbO-GeO_2 glasses.

INTRODUCTION

Much recent research of fiber optic materials has involved the development of ultra low loss, long wavelength optical waveguides, which can operate further in the infrared region than the 1.7μm limit of fused silica-based compositions. The potential of germania-based compositions for such devices has been demonstrated since these can operate at wavelengths greater than 3μm with losses as low as 0.01dB/km[1-4]. In order to develop oxide glasses that will shift their infrared transmittance to long wavelengths, large cations with low field strength can be added. Germanate glasses containing lead oxide are most suitable for such optical waveguide materials[5]. Although glass formation has been reported in PbO-GeO_2 system[6-9], very little is known about the structure and properties of such glasses. Topping et al.[7] indicated from the analysis of the molar volume data that the coordination number of some Ge^{4+} ions in the binary glasses changed from 4 to 6 when PbO was added. Recently, Canale et al.[5] discussed the structure and properties of glasses in the binary PbO-GeO_2 and Bi_2O_3 systems on the basis of interpretation of their vibrational spectra and molar volume data. Umesaki[10] reported the radial distribution function (r.d.f.) of glassy and molten $PbGeO_3$ obtained from the X-ray diffraction data, and suggested the structural model based on PbO_4 pyramid and network forming GeO_4 tetrahedra.

In the present work, in order to clarify the atomic scale structure of glasses in the binary PbO-GeO_2 system, we performed high resolution neutron diffraction measurements on three lead germanate glasses with the compositions $PbO \cdot 4GeO_2$, $PbO \cdot 2GeO_2$ and $2PbO \cdot 3GeO_2$. The obtained neutron structural data were compared with that of vitreous GeO_2 whose structure has been studied previously by Desa et al.[11].

EXPERIMENTAL PROCEDURES

Preparation of Binary PbO-GeO_2 Glass

Three glass samples in the binary PbO-GeO_2 system were prepared for measurement by quenching from the melt. The glass compositions, their measured densities and the glass dimensions are listed in **Table 1**. The lead monoxide used was BHC Chemical Limited AnalaR

Table 1 Rod radii and densities of PbO-GeO_2 glass samples.

Glass composition	Melting Temperature (°C)	Melting Time (hours)	Rod diameter (cm)	Density (c.u.Å^{-3})
GeO_2[11]	1200, 1400	6, 4	5.261	0.0209905
$PbO \cdot 4GeO_2$	1350	4	5.291	0.0048194
$PbO \cdot 2GeO_2$	1140, 1040	4, 1	5.530	0.0078622
$2PbO \cdot 3GeO_2$	1120	3	5.521	0.0047144

PbO quoted 99% purity. The germanium oxide used was Koch-Light GeO_2 quoted at 99.999% purity. Appropriate proportions of PbO and GeO_2 powders were ground in propan-2-ol to aid homogeneous mixing using an agent pestle and mortar. The mixture was put in a platinum crucible and melted. The alcohol evaporated and the resulting melt was clear and appeared to be homogeneously mixed. The PbO-GeO_2 melts were quenched by pouring into 5mm internal diameter steel chill. This chill was warmed to approximately 150°C and casting surfaces were highly polished. This was done to reduce the internal and surface stress in the glass rod. The rod was quickly removed and allowed to cool inside a split pyr muffle.

Neutron Diffraction

1. Theory

The quantity measured in a neutron diffraction experiment is the differential cross-section

$$\frac{d\sigma}{d\Omega} = I^S(Q) + i(Q) \qquad (1)$$

where Q is the momentum transfer, $I^S(Q)$ is the self scattering term and i(Q) is the distinct scattering term. The self scattering, which can be calculated within an approximation, is subtracted from the data to give the distinct scattering. Structural information may then be obtained by using a Fourier transform of the experimental interference function $Q \cdot i(Q)$ to obtain the total correlation function

$$T(r) = T^0(r) + \frac{2}{r}\int_0^\infty Q \cdot i(Q) M(Q) \sin(rQ) dQ \qquad (2)$$

where $T^0(r) = 4\pi g^0\left(\sum c_i \bar{b}_i\right)^2$ is the average density contribution, and M(Q) is a modification function used to take into account the maximum experimentally attainable value of Q.

2. Experimental

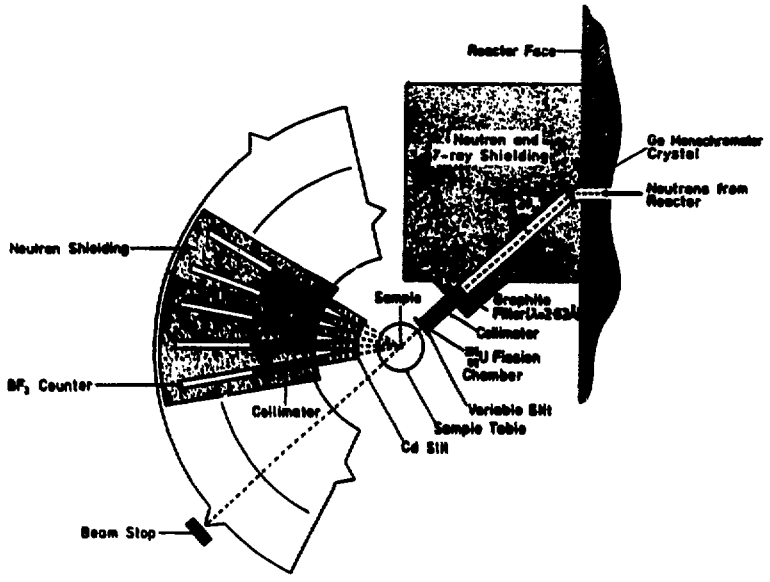

Fig. 1 The CURRAN diffractometer at the Harwell A.E.R.E..

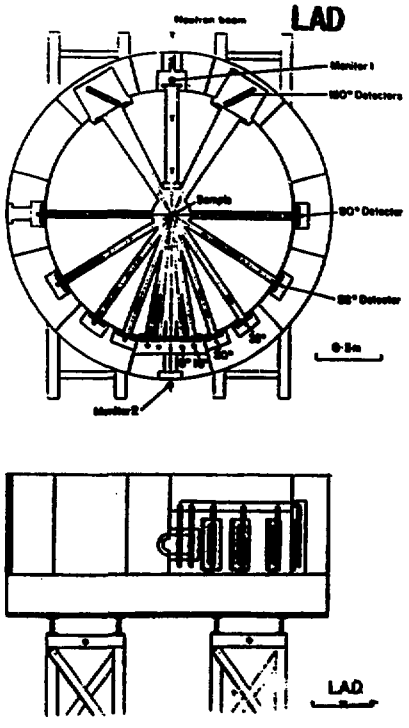

Fig. 2 The LAD diffractometer at the Rutherford Appleton Laboratory.

The neutron experiments employed the same combination of the DIDO CURRAN at Harwell A.E.R.E (see **Fig. 1**) and the Liquid and Amorphous material Diffractometer (LAD) on 800MeV proton synchrotron spallation pulsed source ISIS at the Rutherford Appleton Laboratory (see **Fig. 2**). The CURRAN is a conventional twin axis diffractometer using a monochromatic beam of thermal neutrons, and the CURRAN data are usually more reliable in the low Q region. The LAD diffractometer uses the time-of-flight method, thus enabling very high Q-values to be achieved.

The CURRAN scattering data were obtained for the three glass samples, $PbO \cdot 4GeO_2$, $PbO \cdot 2GeO_2$ and $2PbO \cdot 3GeO_2$, at an incident wavelength of 1.372Å ($0.13 \leq Q \leq 7.39 Å^{-1}$). A vanadium standard (4.77±0.22mm diameter rod) and the empty sample position run were also done to perform the normalization and background correction. The neutron scattering lengths, b, for Ge, O and Pb were taken to be 0.81858×10^{-14}m, 0.5804×10^{-14}m and 0.94003×10^{-14}m respectively. The obtained intensity data were normalized to the vanadium run and re-normalized using the Krogh-Moe-Norman technique. A cubic spline function was fitted to the normalized intensity data and the first diffraction peak was plotted out and extrapolated to $Q=0Å^{-1}$. The experimental interference function $Q \cdot i(Q)$, which represents the diffraction properties of a sample in reciprocal space, was obtained from these smoothed intensity data.

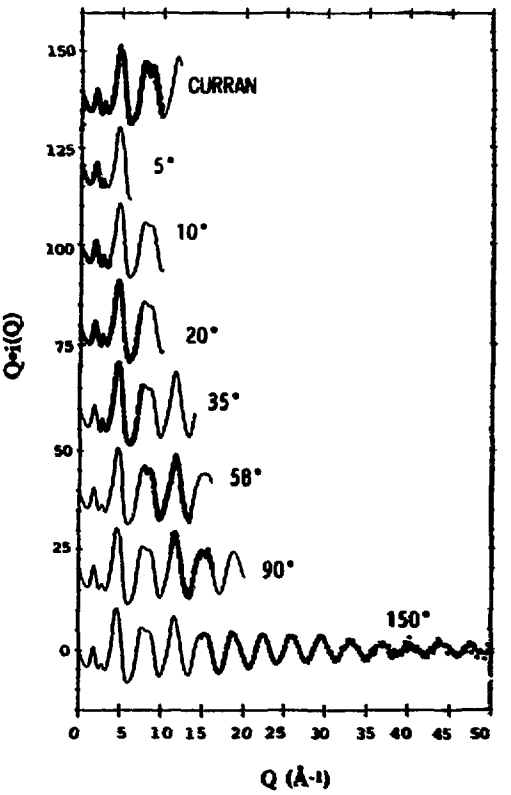

Fig. 3 Interference functions $Q \cdot i(Q)$ for CURRAN and LAD counters on spline fit $PbO \cdot 4GeO_2$ glass.

The LAD experiment involved collecting data from the same three glass samples as used in the CURRAN experiments. In addition, data were collected on vitreous GeO_2. Data on each sample were collected as well as on a 6mm vanadium rod and an empty sample position. The sample: vanadium: background monitor ratio was set at 10: 10: 1. The background spectrum was subtracted from the sample and vanadium spectra and time of flight scale was converted to Q. The Q conversion was performed using the LAD analysis routines written at ISIS and the initial delay is constant, not a function of wavelength. Each vanadium spectrum from all the counters was fitted with a cubic spline function to extract the first derivative of the incident spectrum. The Placzek correction was applied to the vanadium and the new spectrum and first derivative were calculated by fitting a cubic spline again. The spectrum and derivative were used to normalize the sample spectra and perform the Placzek correction. The composition unit ratios were adjusted so that the corrected diffraction patterns for each counter oscillated evenly about the calculated self scattering. To use the superior count statistics of the 150° counters, a polynomial was fitted to $I(Q)$ to emulate the self scattering. The composition unit ratios were adjusted by no more than 5%.

The twin axis data from CURRAN were plotted on a large scale with each counter of the time-of-flight LAD data to check the normalization of the LAD data and to obtain the regions of

best reliability for each counter. The low angle counters (5°, 10°) were excellent agreement with the CURRAN data. The high Q data were taken from the higher angle counters where the data appeared to be most reliable. The combined CURRAN and LAD Q•i(Q) curves of the $PbO \cdot 4GeO_2$ glass are shown in **Fig. 3**. **Fig 4** indicates the resulting Q•i(Q) curve. As shown in this figure, oscillation in the $PbO \cdot 4GeO_2$ glass extended to $50Å^{-1}$.

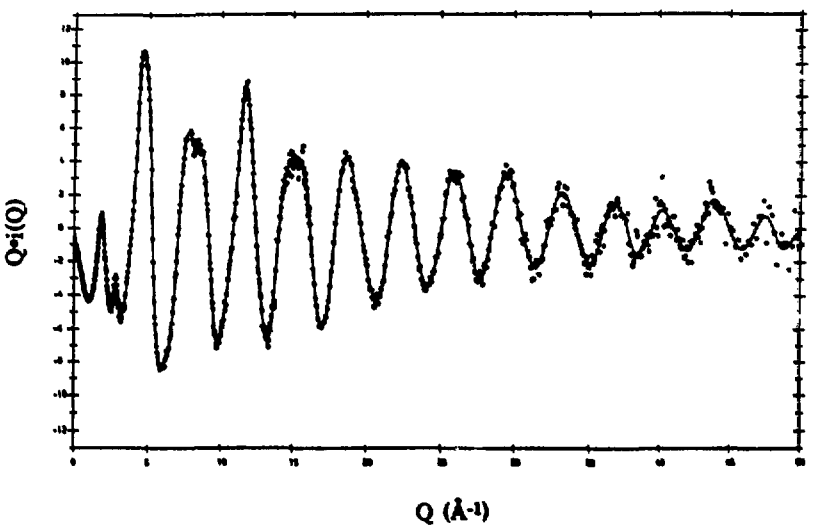

Fig. 4 Interference function Q•i(Q) on spline fit $PbO \cdot 4GeO_2$ glass.

RESULTS AND DISCUSSION

The total correlation functions T(r) were calculated for each of the $PbO\text{-}GeO_2$ glasses from the obtained Q•i(Q) curves and are illustrated in **Fig. 5**. On addition of PbO, several interesting features are apparent. The wavelengths of the high Q oscillations in Q•i(Q) curve tend to decrease with increasing PbO content as does the magnitude of these oscillations. This implies a peak shift in the first peak of T(r) curve along with a decrease in its intensity as shown in Fig. 5. Other features that are altered are a peak at 2.3Å which increases with increasing PbO content, a small shift in the peak at 2.8Å a decreasing of the 3.3Å and 4.4Å peaks.

The peak at 2.3Å can be identified as the first Pb-O distance from corresponding distances in the PbO crystal structures (yellow PbO[12] implies Pb-O bond length = 2.2-2.4Å, and red PbO[13] implies Pb-O bond length = 2.34Å). The O-O peak at 2.8Å tends to shift slightly to higher r. This could be due to either the formation of GeO_6 octahedra or the O-O distance in the PbO_4 tetrahedra. In order to look at the structural feature in the obtained T(r) curves in more detail, we may consider the difference function i.e. $PbO\text{-}GeO_2$ T(r) minus GeO_2 T(r) as shown in **Fig. 6**. These correction functions have been normalized so that each composition unit contains one GeO_2 unit. The most striking feature in these curves is the growth of a sharp contribution on the falling edge of the first Ge-O peak. This peak is positioned at 1.9Å which indicates a structure related to the rutile form of germania crystal. Rutile GeO_2 is composed of GeO_6 octahedra as opposed to GeO_4 tetrahedra as is found in the pure vitreous GeO_2. The Ge-O distance in this form is 1.872Å to 1.902Å. This peak grows with increasing PbO.

Peak fits were performed for the measured $PbO\text{-}GeO_2$ glasses and the parameters for these fits are given in **Table 2**. It can be seen that the Ge-O coordination number increases with increasing PbO which again indicates the presence of a more highly coordinated structural unit (GeO_6 octahedra). The value of the coordination number for the highest lead content glass

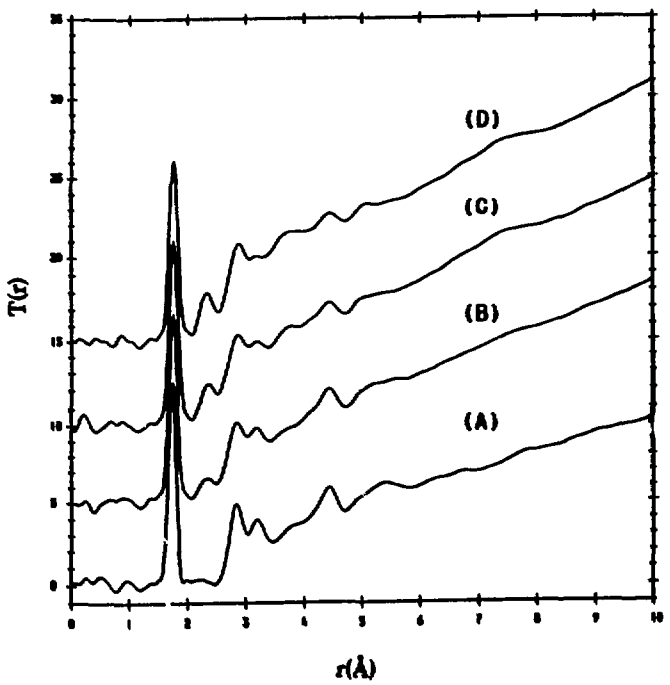

Fig. 5 Total correlation functions T(r) for (A) GeO_2, (B) $PbO \cdot 4GeO_2$, (C)$PbO \cdot 2GeO_2$ and $2PbO \cdot 3GeO_2$ glasses.

Table 2 Peak fit parameters for $PbO\text{-}GeO_2$ glasses.

	Peak	r_{jk} (Å)	u_{jk}^2 (Å^2)	n_{jk} (atoms)
GeO_2 glass (Q_{max}=58Å^{-1})	Ge-O	1.742±0.002	0.045±0.002	3.74±0.08
	O-O	2.839±0.008	0.111±0.007	5.87±0.28
GeO_2 glass (Q_{max}=42Å^{-1})	Ge-O	1.741±0.002	0.047±0.002	3.78±0.08
	O-O	2.840±0.009	0.113±0.007	5.93±0.28
$PbO \cdot 4GeO_2$ glass (Q_{max}=42Å^{-1})	Ge-O(4)	1.7500±0.0006	0.0436±0.0007	3.93±0.03
	Ge-O(6)	1.89	0.1	0.53
	Pb-O	2.343±0.007	0.126±0.005	6.28±0.21
$PbO \cdot 2GeO_2$ glass (Q_{max}=42Å^{-1})	Ge-O(4)	1.755±0.001	0.055±0.002	4.00±0.005
	Ge-O(6)	1.89	0.1	0.57
	Pb-O	2.355±0.010	0.123±0.008	6.72±0.32
$2PbO \cdot 3GeO_2$ glass (Q_{max}=42Å^{-1})	Ge-O(4)	1.7572	0.054	4.19
	Ge-O(6)	1.877±0.015	0.112±0.017	0.58±0.05
	Pb-O	2.336±0.006	0.121±0.004	6.23±0.13

Ge-O(4): four-fold coordinated Ge; Ge-O(6): six-fold coordinated Ge
(Coordination numbers njk for Ge-O(6) give the contribution to the remaining area under the peak on the same scaling as Ge-O(4) so both sum to give the total coordination numbers.)

$2PbO \cdot 3GeO_2$ was 4.77 which implies that the ratio of six-fold coordinated Ge to four-fold coordinated Ge is approximately 1:3. This agrees with the estimated ratio in $Na_2O\text{-}GeO_2$ glasses

by X-ray diffraction[14] at the minimum in the germanate anomaly (1:3). Thus the fact that the anomaly is stronger in alkali germanate glasses is probably due to the network formation of the PbO reducing the overall packing efficiency.

It is difficult to say exactly in what form the PbO exits in the germanate glasses but some indication is given by comparison with its crystal polymorphs. Lead oxide exists in two crystal forms; red lead oxide Pb_3O_4 exists in bimolecular tetragonal units and yellow lead oxide PbO is orthorhombic. The values for the Pb-O distance are 2.33Å for tetragonal structure and 2.21Å to 2.42Å in the orthorhombic structure. Close inspection of the T(r) difference functions shows that the Pb-O peak is positioned at 2.33Å but its broadness indicates that the orthorhombic structure cannot be ruled out. The Pb-Pb distances found in the crystal polymorphs are 3.70-3.90Å in the tetragonal structure and 3.47-3.63Å in the orthorhombic structure. As shown in Fig.6, inspection of the difference functions shows a peak positioned at 3.55Å increasing in intensity with increasing PbO content which would suggest that this feature is due to the Pb-Pb correlations. The range defined by tetragonal PbO covers a minimum in the ($PbO \cdot 4GeO_2$-GeO_2) function and it is therefore very unlikely that this structural unit is occurring in the PbO-GeO_2 glasses. The peak maximum is close to the center of the range covered by the orthorhombic PbO Pb-Pb distance, and therefore it is reasonable to conclude that the PbO could exist as it does in orthorhombic PbO i.e. as pyramids of PbO_4^{2-} with all oxygens on one side of the Pb atom, one pair spaced at 2.21Å from the Pb atom and the other at 2.42Å. The coordination number for Pb-O correlation in the PbO-GeO_2 glasses is approximately 6. This is the value expected for the orthorhombic PbO (as opposed to 3 in tetragonal Pb_3O_4) which would agree with the previous points.

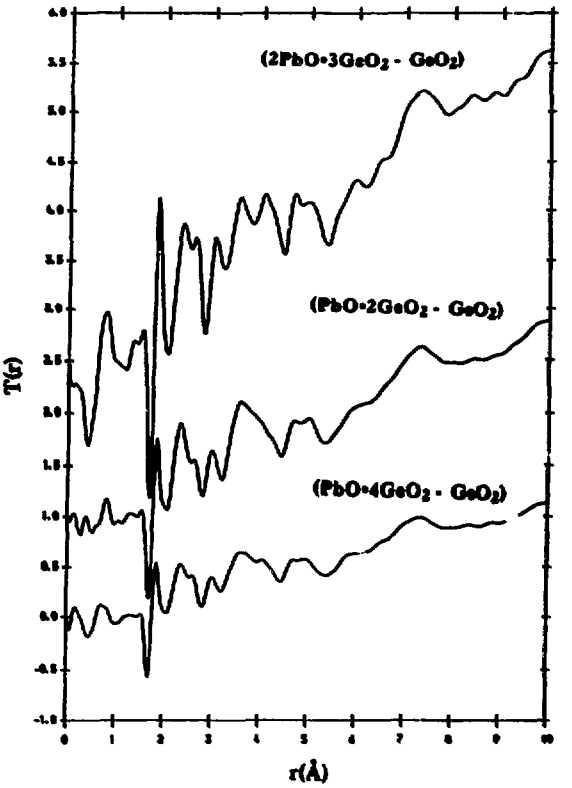

Fig. 6 Difference correlation functions T(r) for ($2PbO \cdot 3GeO_2$-GeO_2), ($PbO \cdot GeO_2$ -GeO_2) and ($PbO \cdot 4GeO_2$-GeO_2).

REFERENCES

1) K. Nassau, D.L. Wood and D.L. Chadwick: Appl. Optics, **21** (1982) 4276.
2) K. Nassau: The Bell Syst. Tech. J., **60** (1981) 327.
3) K. Nassau and D.L. Chadwick: J. Am. Ceram. Soc., **65** (1982) 486.
4) K. Nassau and D.L. Chadwick: J. Am. Ceram Soc., **65** (1982) 195.
5) J.E. Canale, R.A. Condrate, Sr.K. Nassau and B.C. Cornilsen: J. Can. Ceram. Soc., **55** (1986) 50.
6) O.V. Mazurin, M.V. Strel'tsina and T.P. Shvaiko-Shvaikoskaya: Properties of Glasses and Glass-Forming Melts, Vol. III, Izdatel'stvo Nauka, Leningrade, 1973.
7) J.A. Topping, I.T. Harrower and M.K. Murthy: J. Am. Ceram Soc., **57** (1974) 209.

8) M. Imaoka: J. Ceram. Assoc. Jpn., **67** (1959) 364.
9) J.E. Shelby: J. Am. Ceram. Soc., **66** (1983) 414.
10) N. Umesaki: Doctoral Thesis (Osaka Univ., 1981, p.53-69).
11) J.A.E. Desa, A.C. Wright and R.N. Sinclair: J. Non-Cryst. Solids, **51** (1982) 57.
12) R. Soderquist and B. Dickens: J. Phys. Chem. Solids, **28** (1967) 823.
13) B. Dickens: J. Inorg. Nucl. Chem., **27** (1965) 1503, 1495.
14) K. Kamiya and S. Sakka: Phys. Chem. Glasses, **20** (1979) 60